Materials Research Bulletin 157 (2023) 112034

Contents lists available at ScienceDirect

Materials Research Bulletin

journal homepage: www.elsevier.com/locate/matresbu

Research Papers

Dielectric, ferroelectric and electrocaloric properties of 1%Eu - doped $BaZr_yTi_{1-y}O_3$ ceramics

Lavinia Curecheriu [a,*], Teodora Sandu [a], Oana Condurache [a,b], Giovanna Canu [c], Chiara Costa [c], Maria Teresa Buscaglia [c], Mihai Asandulesa [d], Juras Banys [e], Vincenzo Buscaglia [c], Liliana Mitoseriu [a,*]

[a] Dielectrics, Ferroelectrics & Multiferroics Group, Faculty of Physics, "Al. I. Cuza" University, Blvd. Carol I, no.11, Iasi 700506, Romania
[b] Electronic Ceramics Department, Jožef Stefan Institute, Jamova 39, Ljubljana 1000, Slovenia
[c] Institute of Condensed Matter Chemistry & Technologies for Energy, CNR, Via De Marini 6, Genoa I-16149, Italy
[d] Petru Poni" Institute of Macromolecular Chemistry, Aleea Grigore Ghica Voda 41A, Iasi 700487, Romania
[e] Faculty of Physics, Vilnius University, Saulėtekio al. 9, Vilnius LT-10222, Lithuania

ARTICLE INFO

Keywords:
$BaTiO_3$- solid solutions
Dielectric
Dc-tunability
Electrocaloric effect

ABSTRACT

Pure perovskite 1%Eu – $BaZr_yTi_{1-0.0025-y}O_3$ ceramics with compositions $y = 0$, 0.05, 0.15, and 0.30 prepared by solid-state reaction were investigated by impedance spectroscopy and high field measurements (P(E), dc-tunability). The ceramic samples present a nonlinear dielectric character and the dc-tunability reaches a maximum for $y = 0.15$ ($n_r = 85\%$) due to the proximity of the ferroelectric-paraelectric phase transition and due to a good accommodation of the europium ions into the BZT matrix. All the compositions have a maximum temperature change around the phase transition with a maximum ΔT=1.13 K for $y = 0$. At room temperature, the maximum is found for the composition $y = 0.05$ (ΔT=0.46 K), while for $y = 0.15$ a constant value ΔT=0.40 K was obtained from room temperature up to 350 K. This kind of electrocaloric dependence, the large nonlinear dielectric character with the lack of hysteresis in the permittivity vs. field dependence make this composition as interesting for microelectronics applications.

1. Introduction

The continuous miniaturization of modern electronic devices demands nowadays for new strategies to limit the devices overheating during their current use. Based on the adiabatic demagnetization or depolarization cooling, a new type of solid-state refrigeration technique was proposed in the last years. The depolarization cooling denoted as electrocaloric refrigeration uses the electrocaloric effect of ferroelectrics [1,2]. The electrocaloric (EC) effect is determined by the change of polarization states when an external electric field is applied to or removed from a polar material under adiabatic conditions. Concerning other types of cooling techniques for example ones using large magnetocaloric solid-state refrigerators, the main advantage of electrocaloric (EC) refrigeration is their reduced size and the possibility of device downscaling [3,4]. This is beneficial for its applications in cooling microelectronic chips. The main problem in the design of solid-state cooling devices is to find materials with high and stable EC effect around room temperature. Some of the promising candidates seem to be ferroelectrics or relaxors, due to their large polarization and their field and temperature-induced structural transformations. The study of EC materials knew a revival of interest in 2006 after the paper of Mischenko et al. that reported for Pb(Zr, Ti)O_3 thin films the largest ever found adiabatic temperature change of ΔT=12 K at 499 K, under an external field of 480 kV/cm [5]. Other authors reported various significant EC performances for different combinations of ferroelectrics or ferroelectric-relaxors, for example, ΔT=2.7 K at 492 K under 90 kV/cm in 0.7PMN-0.3PT bulk ceramics [6] or 40 K at 318 K under 1200 kV/cm in PLZT thin films [7].

For developing cooling devices containing such ferroelectrics, it is necessary to find materials operating at rather low fields, in a large temperature range near room temperature [8–11]. Another challenge is related to the fact that the largest number of ferroelectrics and relaxor oxides currently used as EC materials are Pb-based ceramics. The increased interest in developing lead-free ferroelectrics was recently

* Corresponding authors.
E-mail addresses: lavinia.curecheriu@uaic.ro (L. Curecheriu), lmtsr@uaic.ro (L. Mitoseriu).

https://doi.org/10.1016/j.materresbull.2022.112034
Received 17 March 2022; Received in revised form 5 September 2022; Accepted 13 September 2022
Available online 15 September 2022

determined by environmental regulations, which became increasingly more stringent in the view of eliminating the use of lead in microelectronics [12]. A few families of solid solutions were proposed as possible candidates to replace lead zirconate titanate (PZT) in EC applications, mainly based on: (K, Na)NbO_3, $Bi_{1/2}Na_{1/2}TiO_3$ or $BaTiO_3$ (BT) solid solutions [13]. Among them, the BT family has been extensively tested for EC properties in all forms: single crystals, thin films (also in multilayer ceramic capacitor structures), or bulk ceramics [14–18]. A large ΔT has been reported for BT-ceramics in the vicinity of their ferroelectric-paraelectric (FE-PE) (tetragonal-cubic T-C) phase transition [14]. It is noted that besides the T-C transition, the BT family may also exhibit orthorhombic (O) or rhombohedral (R) structural phases. Because the EC effect is related to the variation of entropy induced by the electric field modifications, a ferroelectric in which multiple polarization orientations can be produced under the application of an accessible electric field could promote a large ΔT. Furthermore, a high EC effect can be easily induced under a small electric field input if the energy barriers for switching between the polar states are smaller [19]. For BT-based materials, the existing six equivalent polar-states in the FE phase and a large permittivity increase at the FE-PE transition determine a strong ΔT/ ΔE for temperatures above the phase transformation, as was shown in the single crystal and ceramics [20]. Due to the high FE-PE transition temperature (T_C=120 °C), the use of pure BT as EC materials is limited, but the Curie temperature can be easily tailored by the incorporation of suitable dopants [21]. The substitution of Ti^{4+} with various types of homovalent ions M^{4+} (where M^{4+}=Zr, Ce, Sn, Hf) and the formation of $BaM_yTi_{1-y}O_3$ solid solutions have attracted large attention from both fundamental and applicative points of view [22, 23]. When increasing the concentration of M^{4+}, a shift from a classical ferroelectric to a relaxor state usually occurs. When using Zr^{4+} substitution in $BaZr_yTi_{1-y}O_3$ (BZT) solid solution, if y<0.08, the system has a ferroelectric character, while for larger y, BZT shows a progressive broadening of the ε (T) dependence, caused by the local inhomogeneous distribution of Zr^{4+} ions among the Ti^{4+} sites and of the inhomogeneous local stress inside the ceramic grains. For $y < 0.10$, the increase of y determines an increase in the temperatures corresponding to both R-O and O-T, as well as a decrease in the T-C phase transition temperature [24]. The transition temperatures continue to approach each other by the further increase of y, until for a certain Zr content, a pinched single transition is observed. According to Verbitskaya et al. [25], for the compositions in the range $0.10 < y \leq 0.15$, a diffuse phase transition with a mixture of rhombohedral, tetragonal, and cubic phase occurs at room temperature, for which twenty-six polarization states are allowed [26], that may lead to a significant increase of the non-polar phase entropy and consequently, to a higher ΔT.

On the other hand, the rare earth (RE) doping of $BaTiO_3$-based ferroelectrics provides advantages such as long-term reliability in resistance degradation, grain size refinement, high-permittivity behavior, and dielectric-temperature stability [27,28]. The presence of RE ions can provide modifications of lattice symmetry and grain size in ceramics, which are important factors modifying the electrical properties. In particular, doping with small amounts of rare earth oxides can inhibit irregular grain growth, promote better ceramic densification and improve the dielectric properties [29]. The role of rare-earth doping on the structural and dielectric properties of $BaTiO_3$ - based solid solution has been studied mainly by using La, Ce, Dy [27,28], while only a few papers reported investigations concerning the low field dielectric properties and conductivity dispersion properties of Eu-doped BZT ceramics [30, 31] and the role of various types of RE on tunability characteristics were reported in ref. [32]. All the mentioned papers mostly analyzed the role of RE doping level, none of them tested ferroelectric hysteresis loops as a function of temperature and EC effect or detailed non-linear dielectric properties. Europium may exist as metastable Eu^{2+} ions with a half-filled 4f [33] shell or with mixed Eu^{2+}/Eu^{3+} oxidation states [34]. Small Eu substitutions usually replace Ba ions in the perovskite cell (thus acting as donors), which may change the order-disorder and local symmetry in the matrix and modify the optoelectronic, relaxor character and increase the volume resistivity of $BaTiO_3$-based ceramics through the creation of Ti vacancies for charge compensation [35,36]. The presence of Eu ions may act as an activator for host materials, and it was mostly explored for luminescent properties [37]. However, besides optical characteristics which were previously reported, the literature survey indicated that there is still space for exploring the dielectric, ferroelectric, tunability and electrocaloric properties of BZT ceramics with different Zr contents and a low Eu doping level, by considering the microstructural improvements promoted by the presence of this rare earth ions.

In the present work, 1% Eu - doped $BaZr_yTi_{1-y}O_3$ (with variable Zr level: y = 0, 0.05, 0.15 and 0.30) ceramics prepared by classical solid-state reaction were investigated. The powders were sintered at a temperature of 1500°C to promote the incorporation of Eu^{3+}ions on Ba sites and of Zr^{4+} ions onto Ti sites. The effect of Zr addition on the functional properties (dielectric, dc-tunability, ferroelectric switching at different temperatures and electrocaloric effect) was tested and discussed.

2. Materials and methods

$Ba_{0.99}Eu_{0.01}Zr_yTi_{1-0.0025-y}O_3$ (1%Eu - BZT) ceramics with various compositions: y = 0, 0.05, 0.15 and 0.30 have been prepared by solid state reaction. The chosen compositions correspond to Eu^{3+} substitution at the Ba site with Ti vacancy compensation. The starting raw materials were $BaCO_3$ (Solvay, 99.9% purity), TiO_2 (Degussa, 99.9% purity), ZrO_2 (Toho, 99.9%), and Eu_2O_3 (Metal Rare Earth Ltd.) nanopowders, which were weighted and mixed with distilled water for 24 h. After freeze-drying, the powders were calcined at 1000 °C for 4 h to promote the formation of the perovskite phase. The calcined powders were sieved, and the resulted powders were compacted in cylinders by cold isostatic pressing at 1500 bar and then sintered at 1500 °C for 4 h. The density of the sintered ceramics was determined by the Archimede's method.

The phase purity of the ceramics was determined using X-ray diffraction (XRD) with CuKα radiation (Panalytical Cubix) with a scan step of 0.02° and a counting time of 7 s/step, for 2θ ranging between 20° and 80° To investigate the morphology of the internal cross-section surfaces of the Eu-$BaZr_yTi_{1-y}O_3$ ceramics, scanning electron microscopy (SEM JEOL JSM 6390 with EDX) was employed.

For the electric measurements, Ag–Pb electrodes were deposited on the polished surfaces of the ceramics followed by annealing in air at 200 °C for 2 h. Permittivity measurements of ceramic samples in the frequency range (20 Hz–100 MHz) and temperatures between 150 and 500 K were performed by adapting the parallel-plate capacitor method using HP 4284 LCR analyzer. Permittivity and the loss tangent in this range were determined from the measured complex impedance. Dc-tunability measurements were performed at room temperature using a homemade set-up as described in Ref. [38]. P(E) hysteresis loops as a function of temperature were measured using a Radiant Precision Multiferroic II Ferroelectric Test System on fresh ceramics with a frequency of 10 Hz and a double bipolar voltage as electric input.

3. Results and discussion

3.1. Phase and microstructural characterization

Fig. 1 shows the XRD patterns of the 1%Eu - BZT ceramics, for different Zr content, y = 0, 0.05, 0.15, and 0.30 after sintering at 1500 °C/4 h. The lack of any Ba, Eu, Ti, or Zr-rich secondary phases in the XRD detection limit demonstrates that the solid-state reactions took place, and the incorporation of Eu and Zr in the perovskite lattice was complete. It can be observed that the substitution of Zr^{4+} (ionic radius 0.84 Å) into Ti^{4+}place (ionic radius 0.74 Å) changes gradually the crystalline symmetry of the homogeneous solid solutions. As reported in previous studies [39–41], BZT may have orthorhombic, rhombohedral, and tetragonal structures at room temperature, depending upon the Zr

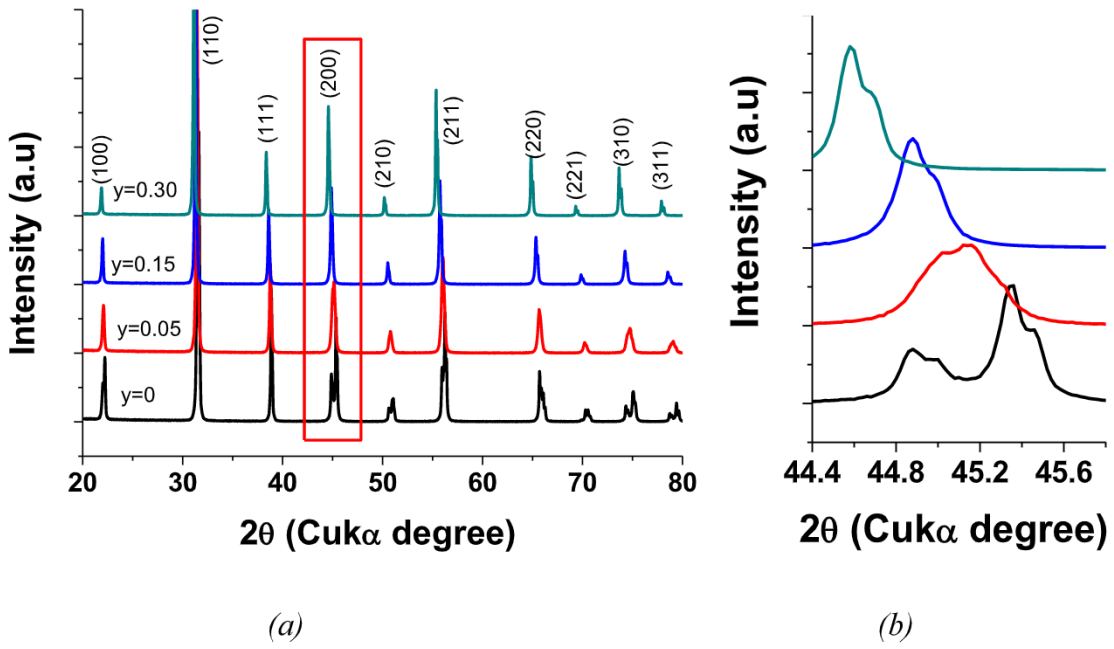

Fig. 1. (a) XRD patterns at room temperature for 1%Eu - BZT ceramics sintered at 1500°C/4 h; (b) Magnified representation for 2θ range corresponding to the (200)-(002) reflections.of the range (red rectangle of Fig. 1(a)) for

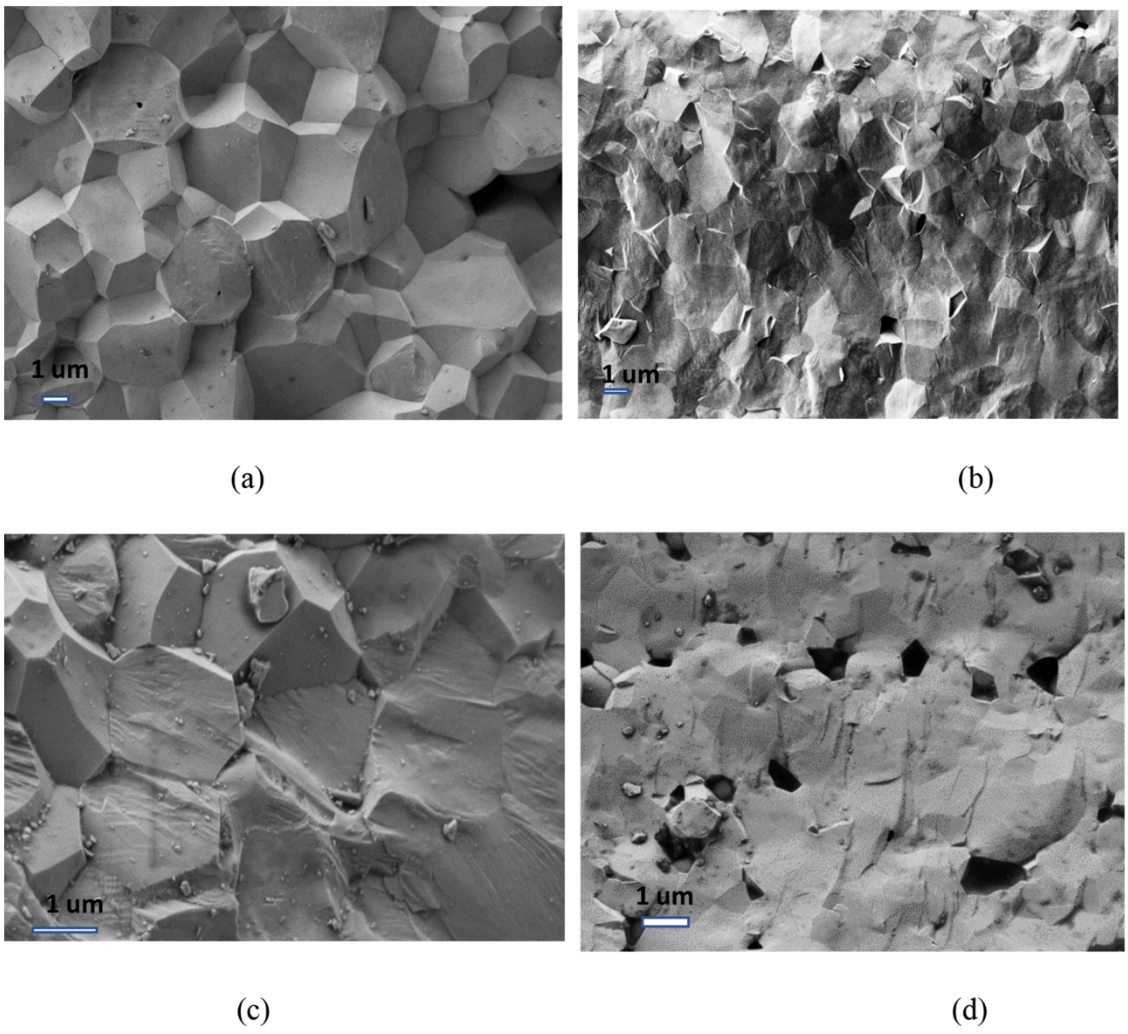

Fig. 2. SEM images on fresh fractured surfaces of 1%Eu - BZT ceramics sintered at 1500°C / 4hours: (a) $y = 0$; (b) $y = 0.05$; (c) $y = 0.15$; (d) $y = 0.30$.

content. In our case, ceramic with $y = 0$ shows a tetragonal structure with a (200)-(002) peak splitting around $2\theta \sim 45°$, while for increasing Zr content a superposition of orthorhombic and tetragonal states was observed for $y = 0.05$, and a pseudo-cubic structure, with a single diffraction peak around 45° for $y = 0.15$ and 0.30. The inset of Fig. 1(b) emphasized the structural modification and the shift of the (200)-(002) reflections toward lower values of diffraction angle when increasing Zr content, due to the larger cell volume induced by the gradual incorporation of Zr^{4+} onto the Ti^{4+} sites [41]. A detailed structural analysis with Rietveld refinement showing the variation of the c/a tetragonal ratio and of unit cell volume vs. Zr addition was performed in our previous paper [37].

.Dense and uniform ceramic microstructures with faceted grains well interconnected and often perfect triple points, for all investigated compositions, are observed in the SEM images collected on the freshly fractured surfaces (Fig. 2a-d). Among the investigated solid solutions, a higher intergranular porosity is typical to the composition with the highest Zr level, $y = 0.30$. This is confirmed by the obtained relative densities of Eu-BZT sintered ceramics, which assume high values of: 96%, 99%, 99.9%, and 94% for $y = 0$, 0.05, 0.15, and 0.30, respectively. For higher Zr additions, better densification could be promoted by using a higher sintering temperature, but in the present study, the same sintering strategy was preferred for all the compositions. The ceramic grain sizes are in the range of about (2–5)μm. Their size is very similar for a given concentration, as result of the presence of Eu doping which was reported to inhibit irregular grain growth and to induce a better densification and providing homogeneous microstructure [29]. With respect to similar undoped BZT compositions sintered in the same temperature range, which presented exaggerated grain growth [42], it is worth to note that the dissolution of 1%Eu^{3+} as donor dopants increases the oxygen vacancies level, which contributes to the overall increase in cationic transport and hence, limiting the grain growth. Therefore, the presence of Eu^{3+} donor dopants reduce the overall diffusion speed during sintering and allows the formation of homogeneous ceramic microstructures.

3.2. Low field dielectric properties

3.2.1. Temperature dependence of the dielectric properties

The evolution with temperature of the real and imaginary parts of permittivity and dielectric loss at $f = 1$ MHz, for the Eu-BZT ceramic samples, is shown in Fig. 3 (a, b, c). The high values of permittivity and low losses below 3% at room temperature (RT) indicate a very good dielectric character for all the compositions. These data revealed a room temperature permittivity of ~ 2000 for the compositions $y = 0$ and $y = 0.30$, ~ 4000 for $y = 0.05$ and above 7500 for $y = 0.15$, (which is a ceramic with almost full densification). The composition $y = 0.15$ shows a strong variation of permittivity with temperature around room

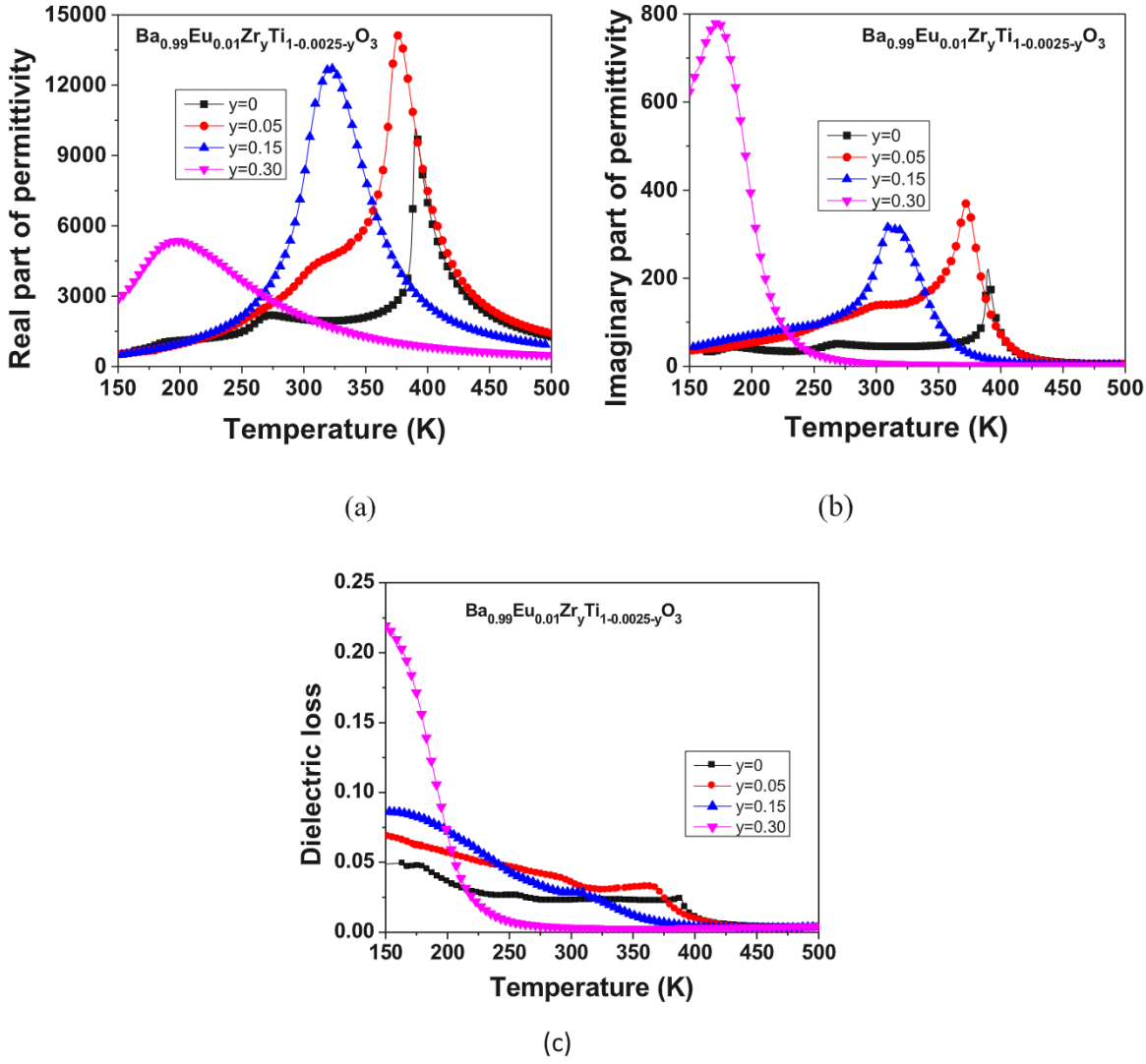

Fig. 3. (a) Real, (b) imaginary part of the dielectric constant and (c) dielectric loss versus temperature at a fixed frequency of 1 MHz, for 1% Eu - BZT ceramics.

temperature due to the proximity of its FE-PE phase transition. The observed anomalies of permittivity vs. temperature indicate that all the structural transitions are detectable only for $y = 0$ at temperatures of 187 K (R-O), 274 K (O-T), and 390 K (T-C), respectively. These transition temperatures are in good agreement with ones usually reported for pure BT ceramics [43] and confirm that small additions of Eu do not change the temperatures corresponding to the structural phase transitions of BT [44]. For the ceramic sample with $y = 0.05$ only two anomalies are observed at 306 K (O-T) and 377 K (T-C), respectively, while $y = 0.15$ presents a single dielectric anomaly at 326 K. The Curie temperature T_C for $y = 0.15$ is smaller than one usually found in the literature for pure BZT ceramics, which was detected in the range of T_C = (333–338) K [45–47], but very close to one reported by Deluca et al. [48] in BZT ceramics having the same compositions but produced from powders synthesized by Pechini route. Therefore, irrespective of the Zr doping level, we may conclude that the addition of only 1% Eu doping does not cause detectable modifications of the corresponding polymorphic transitions characterizing the same compositions of undoped BZT ceramics.

Fig. 3(b) shows the temperature dependence of the imaginary part of permittivity for all the compositions. All the samples have a maximum around the structural phase transitions and decrease to almost zero dispersion for temperatures above the Curie region (in the paraelectric states) for each composition.

Fig. 3(c) shows the dielectric loss with temperature for all ceramics. At low temperatures, the ceramic with $y = 0.30$ show large losses (~20%), but for temperatures above 300 K all the samples have low losses (<5%).

The diffuse phase transition of a ferroelectric material is characterized by (i) a broad dependence of the real part of permittivity with temperature; (ii) a deviation from the Curie-Weiss low in the proximity of the temperature corresponding to the permittivity maximum T_m; (iii) a frequency dispersion in the ferroelectric state and a shift T_m; (iv) no frequency dispersion in the paraelectric state.

Above the Curie temperature ($T>T_C$), the dielectric constant of a ferroelectric is described by the Curie-Weiss law:

$$\frac{1}{\varepsilon} = \frac{T - T_0}{C}, \ (T > T_m) \tag{1}$$

where T_0 is the Curie-Weiss temperature and C is the Curie constant, and both are frequency dependent.

For the present 1%Eu-BZT ceramics, the dielectric constant was fitted with the Curie-Weiss law, to observe the dependence of the fitting parameters on Zr content (Table 1). It is noted that by increasing the Zr addition, a gradual deviation from the Curie-Weiss dependence appears, which is more evident for the sample with higher Zr content, $y = 0.30$. The temperature where deviation from the Curie-Weiss law (T_{CW}) occurs is considered the onset temperature for the appearance of local nano-polar order in the paraelectric state [49]. The parameter $\Delta T_m = T_{CW} - T_m$, used to measure the degree of deviation of the dielectric behavior from the Curie-Weiss law [50], increases when increasing Zr content (Table 1), which evidences a composition-induced diffuse phase-transition behavior in 1%Eu-BZT ceramics with $0.05 < y < 0.30$.

To further explore the diffuse phase transition and relaxor character for the compositions with higher Zr concentrations, a modified Curie-Weiss law was also employed [51]:

$$\varepsilon = \frac{\varepsilon_m}{1 + \left(\frac{T - T_m}{\delta}\right)^{\eta}}, \tag{2}$$

where ε_m is the maximum value of permittivity and T_m is its corresponding temperature. This equation describes the dielectric properties of relaxors for all the temperatures including the dielectric dispersion region [52] and the parameter η describes the diffuseness of the phase transition. For a ferroelectric material η =1 and Curie-Weiss law is obtained, while for systems with completely diffuse phase transition like relaxors show, $\eta = 2$. The δ parameter (which has the dimension of a temperature) indicates the width of the phase transition and is directly correlated with the permittivity broadening temperature range around the ferroelectric – paraelectric transition. The obtained fitting parameters of permittivity data by using eq. (2) are presented in Table 2 for each composition. The crossover from ferroelectric towards relaxor character while increasing Zr content is demonstrated by the increase of both the empirical parameters η (which increases from 1.15 at $y = 0$ to 1.78 at $y = 0.30$) and δ (which increases from 21 at $y = 0$ to 81 at $y = 0.30$). The obtained empirical parameters are like ones determined for undoped BZT with similar concentrations [46,49], which means that the presence of small amounts of 1% Eu does not modify the transformation of BZT ceramics from ferroelectric towards relaxor character with diffuse phase transition when increasing the Zr addition.

3.2.2. Frequency dependence of dielectric properties

The dielectric spectra of the real and imaginary parts of permittivity vs. frequency and temperature at a few selected temperatures of 300 K, 350 K, 450 K, and 500 K, respectively are plotted in Fig. S1 (a-h) – *Supplementary material.* All the compositions present a small variation with frequency of the real part of permittivity, even for high temperatures (T = 500 K) (Figs. S1(a), (c), (e), (g)) and no notable dielectric dispersions are present, as recently reported in Eu-doped $BaZr_{0.05}Ti_{0.95}O_3$ as result of electron compensation trough Ba vacancies during the Eu incorporation into the perovskite lattice [31]. Corroborated with the observation of a single arch in the complex impedance plot of this set of ceramics, it means that the Eu^{3+} substitution at the Ba^{2+} with charge compensation through the formation of Ti vacancies in $Ba_{0.99}Eu_{0.01}Zr_yTi_{1-0.0025-y}O_3$ ceramics does not create charge imbalance or inhomogeneities between the grain core and grain boundaries and provide a good dielectric character with minimum dispersion mechanisms. The dielectric spectra present some specific characteristics in the investigated frequency range of (10^2 Hz – 10^6 Hz): (i) for temperatures around the ferroelectric-paraelectric transformation (300 K and 350 K), all the compositions are stable in frequency; (ii) at higher temperatures (450 K and more evident at 500 K) an increase of both the real and imaginary part of permittivity at low frequencies (10^2–10^4 Hz) is observed, which usually is assigned to Maxwell – Wagner relaxation, possibly associated to the presence of some oxygen vacancies in the sintered ceramics [52] or to inhomogeneous distribution of europium or of Zr/Ti at the ceramic grain boundaries with respect to the volume.

3.3. High field dielectric nonlinearity (Dc-tunability)

Given the good dielectric character and low losses of 1%Eu-BZT ceramics, it was further tested the nonlinear dielectric character under high voltages. The high field dependence of permittivity was measured

Table 1
Curie-Weiss parameters (T_0 - Curie-Weiss temperature, C - Curie constant, and T_{CW} - temperature above which the dielectric constant follows the Curie-Weiss law) were determined from dielectric data collected at 1 MHz.

Composition	$y = 0$	$y = 0.05$	$y = 0.15$	$y = 0.30$
T_0 (K)	377	379	342	261
C (x10^5 K)	1.53	1.70	1.45	1.15
T_{CW} (K)	391	398	360	325
ΔT_m	0	22	38	128

Table 2
The empirical parameters obtained by fitting with eq. (2) of the dielectric data measured at 1 MHz for the 1%Eu - $BaZr_yTi_{1-y}O_3$ ceramics.

Sample	$y = 0$	$y = 0.05$	$y = 0.15$	$y = 0.30$
T_m(K)	391	376	322	197
ε_m	9800	14,151	12,795	5380
η	1.15	1.45	1.71	1.78
δ	21	26	37	81

to explore their characteristics as tunable capacitors. The $\varepsilon(E)$ dependence (dc - tunability) was determined at room temperature at complete increasing/decreasing dc-field cycles (Fig. 4(a)). All the compositions show a strong and non-hysteretic variation of permittivity with the applied electric field, with a tendency towards saturation for fields as high as ~ 30 kV/cm. To eliminate the contributions from possible local charge defects blocked in local energy minima and of possible stresses, all the data were recorded after a few cycles of field increase/decrease (at least 5, after the stabilization of the $\varepsilon(E)$ behavior). The relative tunability of ceramics defined as:

$$n_r = \frac{\varepsilon(0) - \varepsilon(E)}{\varepsilon(0)} \times 100, \quad (3)$$

where $\varepsilon(E)$ is the permittivity measured under the dc field E, while $\varepsilon(0)$ is the zero-field permittivity, varies from 40% for the composition $y = 0$ to 85% for $y = 0.15$, for the same applied field $E = 30$ kV/cm. These tunability values are like ones reported for PMN relaxor ceramics [53] and are in good agreement with ones found in undoped BZT ceramics with the same Zr/Ti amounts [48,54]. It is noted that the largest room temperature tunability (above 85%) is reached for the composition $y = 0.15$, which is a remarkable higher value with respect to ones reported in undoped BZT ceramics [48, 54, 55]. Besides the excellent densification of this composition and grain size homogeneity, which are promoted by the presence of 1%Eu, the main reason for the very high tunability of this composition is related to the proximity of its transition temperature (T_m=327 K) around RT, where all the properties are enhanced due to the lowering of free energy barrier and phase coexistence. This behavior is in accordance with the strong field-dependence of permittivity observed in other $BaTiO_3$ based ceramics [48, 53-56]. Another remarkable result is the relatively high tunability character of the relaxor composition $y = 0.30$, which is similar as one obtained for the ferroelectric composition $y = 0$, but without showing a hysteretic dependence.

With respect to the high field dielectric properties of other RE-doped BZT ceramics [28, 48], where the doping determined a reduced tunability, in the present ceramics with 1%Eu - $BaZr_yTi_{1-y}O_3$ compositions it is observed an improvement of the tunability character [55]. The reason for such tunability increase is most probably related to the microstructural improvements promoted by the presence of small amounts of Eu well accommodated in the crystalline lattice, i.e., better densification, the lack of charge defects and a higher degree of homogeneity within the ceramic volume concerning the local stoichiometry and uniform size and shape of ceramic grains [36].

3.4. Electrocaloric effect

The 1%Eu - $BaZr_yTi_{1-y}O_3$ ceramics are expected to sustain the application of higher voltages due to their abovementioned high density, good dielectric character and low losses and this should be favorable to induce good ferroelectric character and high EC effect, which is higher at larger applied fields. To determine the EC effect there are two types of methods: direct measurements [57] in which the temperature changes are measured directly on the sample and indirect methods in which the entropy changes are obtained from the thermodynamic analysis of the polarization variations with temperature. In the present paper, we used the last one. The hysteresis polarization – field $P(E)$ loops in the ac - regime have been recorded in a broad range of temperatures and the results are presented in Fig. 5. All the compositions show well reproducible $P(E)$ loops at RT due to their high density and low losses. On the other hand, the ferroelectric-relaxor crossover with increasing Zr addition is indicated by the gradual reduction of the loop area, coercive field, saturation, remnant polarization and increasing tilting, i.e., decreasing the rectangularity factor (ratio between the remnant and saturation polarization) [58]. The polarization at the maximum field of 30 kV/cm is in the range of (5–21) $\mu C/cm^2$, which is in good agreement with other values reported for BZT ceramics [55]. A reduction of the remnant polarization from $P_r = 10.6$ $\mu C/cm^2$ to 0.15 $\mu C/cm^2$ and of the coercive field from $E_c = 3.2$ kV/cm to 0.4 kV/cm was observed when increasing the Zr amount from $y = 0$ to 0.30. The composition $y = 0.30$ presents a strongly reduced hysteresis loop and almost linear non-hysteretic behavior, that confirms its relaxor paraelectric state. The coercive field, saturation, and remnant polarization gradually reduce when increased the temperature and the ferroelectric hysteresis loops exhibit almost linear characteristics for all the samples above their T_C (Fig. 5).

Fig. 6 shows the polarization-temperature $P(T)$ plots at a few selected applied electric fields ranging between 0 and 30 kV/cm. By increasing the Zr content, the T_{O-T} and T_C are approaching, and the $P(T)$ dependences manifest a strong decay that flattened with the increase of the applied electric field. Additionally, a modification from a first-order phase transition with a sharper decay of polarization at the Curie temperature to second order is observed with a broad temperature range for which the transition takes place, typically in a $BaTiO_3$-based solid solution with diffuse phase transition [59].

The electrocaloric temperature change (ΔT) was computed from the upper branches of the hysteresis loops by using the following integration:

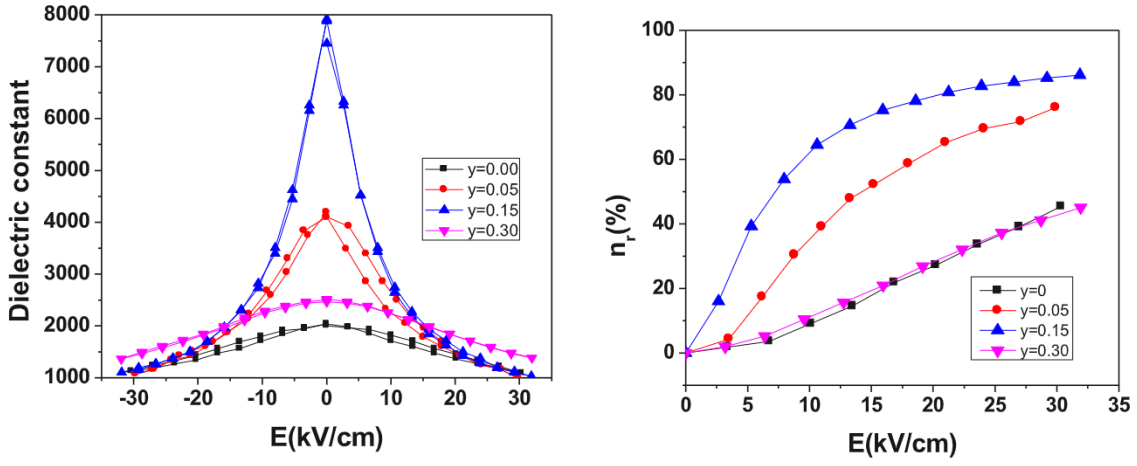

(a) (b)

Fig. 4. Electric field dependence of permittivity and of the relative tunability of 1%Eu - $BaZr_yTi_{1-y}O_3$ ceramics at room temperature.

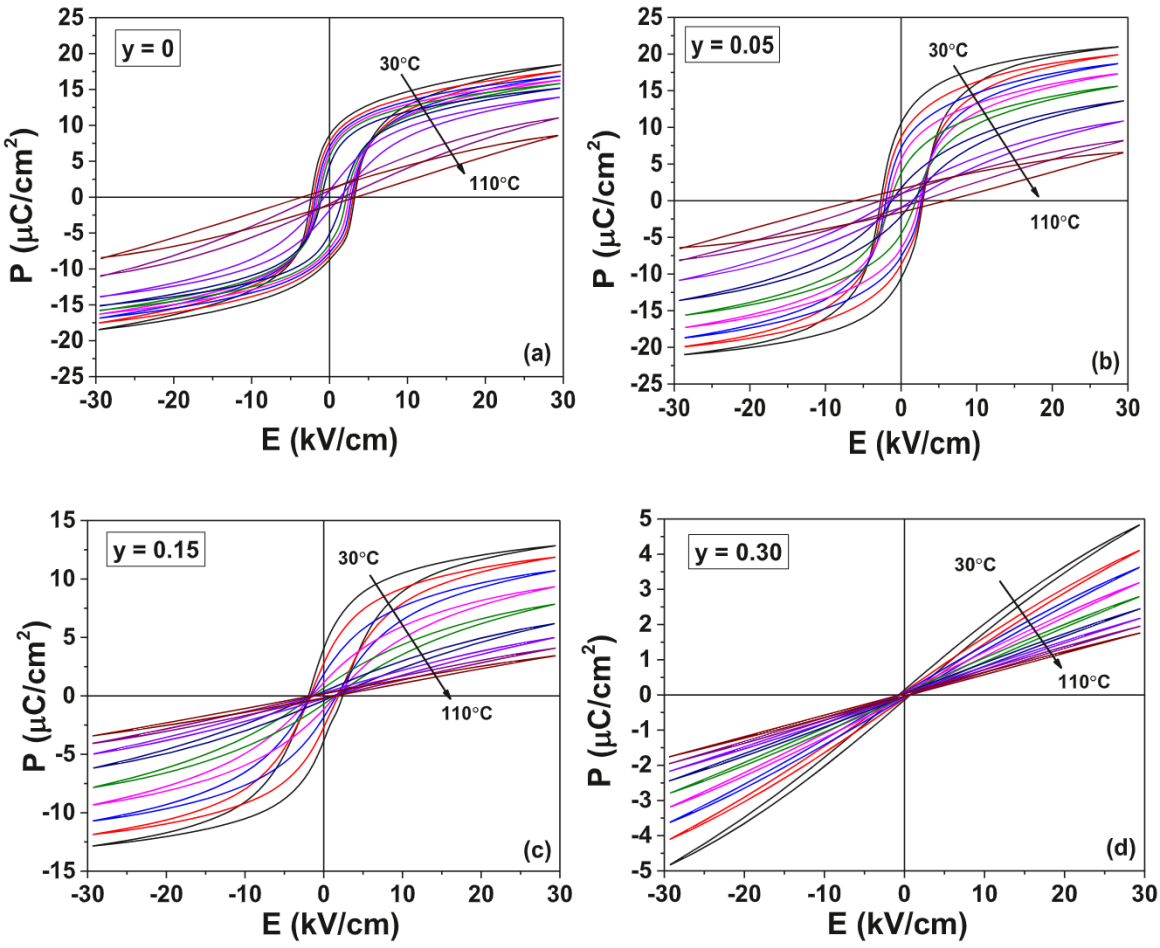

Fig. 5. P(E) loops at few temperatures for 1%Eu - $BaZr_yTi_{1-y}O_3$ ceramics with compositions: (a) $y = 0$, (b) $y = 0.05$, (c) $y = 0.15$ and (d) $y = 0.30$ at $f = 50$ Hz.

$$\Delta T = -\frac{T}{\rho C_E}\int_{E_1}^{E_2}\left(\frac{\partial P}{\partial T}\right)_E E \tag{4}$$

where ρ is the density of the ceramics, C_E is the specific heat capacity at fixed field and E_1 and E_2 represent the limits for the applied electric fields. In our case, $E_1 = 0$, $E_2 = 30$ kV/cm, $\rho = 5.77$ g/cm^3 ($y = 0$), 5.97 g/cm^3 ($y = 0.05$), 6.05 g/cm^3 ($y = 0.15$) and 5.72 g/cm^3 ($y = 0.30$) and C_E was considered according to Ref. [60] as a constant value of 0.50 J/gK for all the compositions.

Fig. 7 shows the calculated dependences of the electrocaloric temperature change ΔT vs. temperature for all the compositions, under $E =$ 30 kV/cm. The sample with $y = 0$ presents the largest ΔT = 1.13 K at 368 K (near its T_C), while the composition $y = 0.05$ has the highest ΔT = 0.45 K at RT, due to the superposition of two ferroelectric polymorphs: orthorhombic and tetragonal. The composition $y = 0.15$ has an almost constant ΔT = 0.40 K from room temperature to $T = 350$ K, due to its multiphase composition. The present results indicate that there is a peak for all the compositions around their own T_C, and a plateau in the case of the ceramic with composition at the tricritical point ($y = 0.15$). For $y =$ 0, a larger electrocaloric temperature change ΔT is found with respect to the case of 2% Eu - doping in $BaTiO_3$ ceramics reported in ref. [60]. The present values are very close to that reported in the literature for pure BZT ceramics [61] and allowed us to conclude that the presence of 1% Eu doping does not damage the electrocaloric properties of BZT ceramics, like in the case 2%Eu-BT [59] and broaden the range with maximum ΔT for $y = 0.15$.

4. Conclusions

$Ba_{0.99}Eu_{0.01}Zr_yTi_{1-0.0025-y}O_3$ (1%Eu - BZT) ceramics were prepared by solid-state reaction and the effect of Zr addition (y) on the dielectric, ferroelectric, dc-tunability and electrocaloric behavior of 1%Eu - BZT were studied. As for undoped BZT ceramics, the Zr substitution modified the structural transition temperature T_m which moved to lower values with increasing Zr content. The room temperature tunability reaches a maximum for $y = 0.15$ ($n_r = 85\%$) due to the proximity of the ferroelectric-paraelectric phase transition and a good accommodation of the europium into the BZT matrix. The highest adiabatic temperature change obtained at room temperature is 0.46 K for $y = 0.05$ and for $y =$ 0.15 a broad range from RT to 350 K with a constant ΔT was obtained. Generally, the presence of Eu in the BZT matrix improved the dielectric properties without creating dielectric dispersion and did not affect the electrocaloric effect concerning ones reported for undoped BZT ceramics. The constant ΔT = 0.40 K for $y = 0.15$ for a broad temperature range from RT to 350 K makes this composition a promising material for application as electrocaloric coolers.

Data availability

Data will be made available on request.

Authors' statement

L.C, L.M, V. B – conceptualization
C.C., G.C, M.T.B – sample preparation
O.C, M.A, J.B – impedance spectroscopy measurements

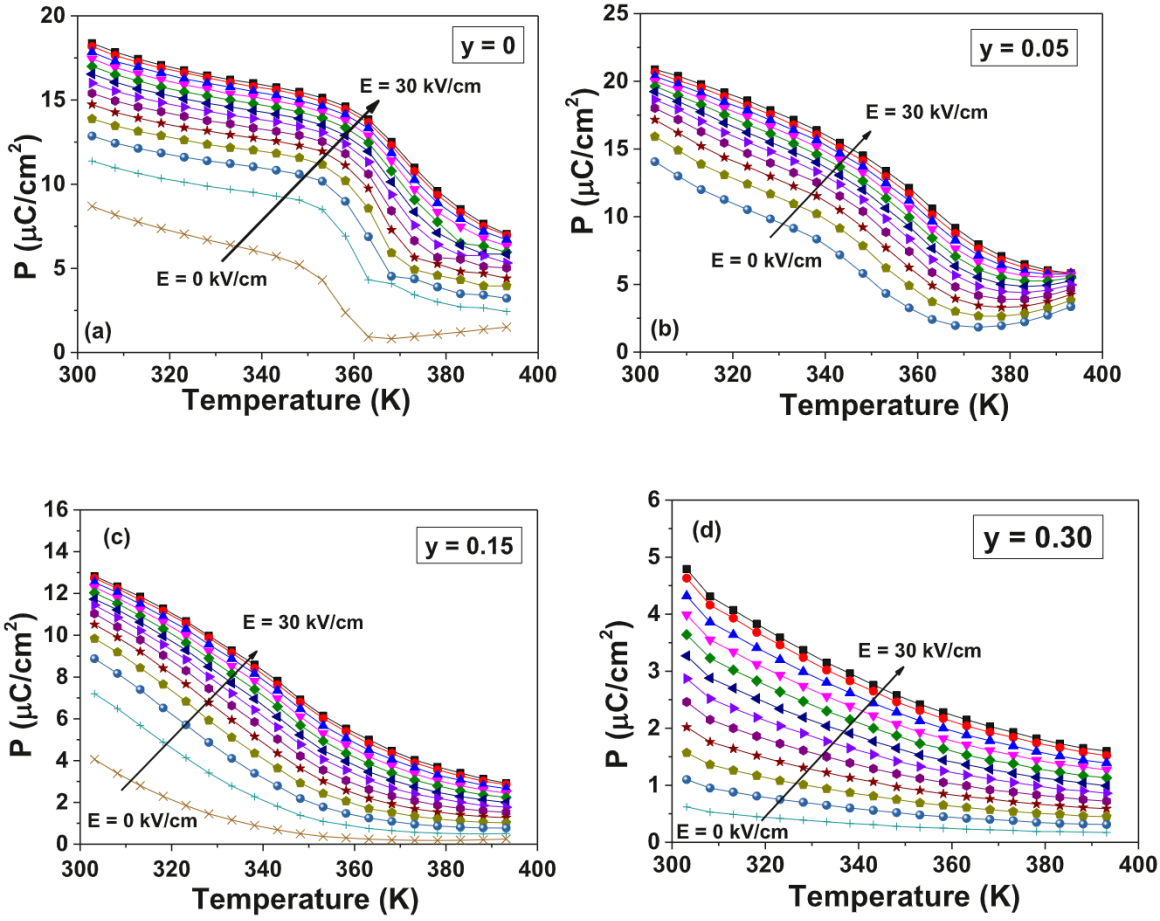

Fig. 6. Polarization vs. temperature for selected applied electric fields for 1%Eu - $BaZr_yTi_{1-y}O_3$ ceramics with compositions: (a) $y = 0$, (b) $y = 0.05$, (c) $y = 0.15$ and (d) $y = 0.30$.

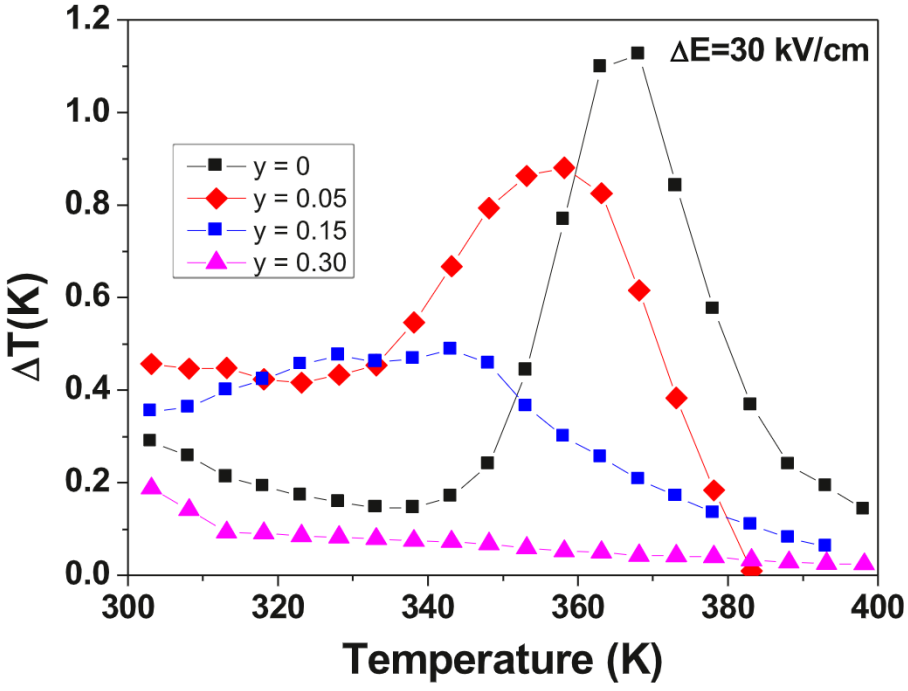

Fig. 7. The temperature dependence of electrocaloric temperature change (ΔT) for 1%Eu - BZT ceramics at ΔE=30 kV/cm.

L.C and T.S – high field measurements (dc-tunability, P(E) loops, electrocaloric measurements, and calculation

L.C and L.M – writing the original draft

Declaration of Competing Interest

The authors declare that they have no known competing financial interests or personal relationships that could have appeared to influence the work reported in this paper.

The authors declare the following financial interests/personal relationships which may be considered as potential competing interests.

Data availability

Data will be made available on request.

Acknowledgments

This research work was carried out in the framework of Romanian project UEFISCDI PN-III-P1-1.1-TE-2019-1689 Grant (CritEC) and Italian project MODULA (ID ROL 34706) funded by the Bank Foundation Compagnia di San Paolo, Torino, Italy.

Supplementary materials

Supplementary material associated with this article can be found, in the online version, at doi:10.1016/j.materresbull.2022.112034.

References

[1] G. Suchaneck, O. Pakhomov, G. Gerlach, Electrocaloric cooling. Refrigeration IntechOpen, 2017.
[2] Cazorla, Simulation of the electrocaloric effect based on first-principles methods, Mater. Sci. (2020).
[3] M. Ozbolt, A. Kitonovski, J. Tusek, A. Poredos, Electrocaloric vs. magnetocaloric energy conversion, Int. J. Refrig. 37 (2014) 16–27.
[4] Y. Meng, Z. Zhang, H. Wu, R. Wu, J. Wu, H. Wang, Q. Pei, A cascade electrocaloric cooling device for large temperature lift, Nat. Energy 5 (2020) 996–1002.
[5] A.S. Mischenko, Q. Zhang, J.F. Scott, R.W. Whatmore, N.D. Mathur, Giant electrocaloric effect in thin-film $PbZr_{0.95}Ti_{0.05}O_3$, Science 311 (2006) 1270.
[6] B. Rozic, M. Kosec, H. Ursic, J. Holc, B. Malic, Q.M. Zhang, R. Blinc, R. Pirc, Z. Kutnjak, Influence of the critical point on the electrocaloric response of relaxor ferroelectrics, J. Appl. Phys. 110 (2011), 064118.
[7] S.G. Lu, B. Rozic, Q.M. Zhang, Z. Kutnjak, X. Li, E. Furman, L.J. Gorny, M. Lin, B. Malic, M. Kosec, R. Blinc, R. Pirc, Organic and inorganic relaxor ferroelectrics with giant electrocaloric effect, Appl. Phys. Lett. 97 (2010), 162904.
[8] P.Loveras Aznar, M. Romanini, M. Barrio, J.-.L. Tamarit, C. Cazorla, D. Errandonea, N. Mathur, A. Planes, X. Moya, L. Manosa, Giant barocaloric effects over a wide temperature range in superionic conductor AgI, Nat. Commm. 8 (2017) 1851.
[9] H. Gu, X.S. Qian, X. Li, B. Craven, W. Zhu, A. Cheng, S.C. Yao, Q.M. Zhang, A chip-scale electrocaloric effect based cooling device, Appl. Phys. Lett. 102 (2013), 122904.
[10] Y. Jia, Y.S. Ju, A solid-state refrigerator based on the electrocaloric effect, Appl. Phys. Lett. 100 (2012), 242901.
[11] X.-.S. Qian, H.-.J. ye, Y.-.T. Zhang, H. Gu, X. Li, C.A. Randall, Q.M. Zhang, Giant electrocaloric response over a broad temperature range in modified $BaTiO_3$ ceramics, Adv. Funct. Mater. 24 (2014) 1300.
[12] European Parliament and the European Council, Off. J. Eur. Union, L.174 (2011) 88.
[13] J. Rodel, W. Jo, K.T.P. Seifert, E.-.M. Anton, T. Granzow, Perspective on the development of lead-free piezoceramics, J. Am. Ceram. Soc. 92 (2009) 1153–1177.
[14] Y. Bai, G.-.P. Zheng, K. Ding, L. Qiao, S.-.Q. Shi, D. Guo, The giant electrocaloric effect and high effective cooling power near room temperature for $BaTiO_3$ thick film, J. Appl, Phys. 110 (2011), 094103.
[15] X. Moya, E. Stern-Taulats, S. Crossley, D. Gonzalez-Alonso, S. Kar-Narayan, A. Planes, L. Manosa, N.D. Mathur, Giant electrocaloric strength in single-crystal $BaTiO_3$, Adv. Mater. 25 (2013) 1360.
[16] X. Niu, X. Jian, X. Chen, H. Li, W. Liang, Y. Yao, T. Tao, B. Liang, S.-.G. Lu, Enhanced electrocaloric effect at room temperature in Mn^{2+} doped lead-free (BaSr)TiO_3 ceramics via a direct measurement, J. Adv. Ceram. 10 (3) (2021) 482–492.
[17] S.P. Beckman, L.F. Wana, J.A. Barra, T. Nishimatsua, Effective hamiltonian methods for predicting the electrocaloric behavior of $BaTiO_3$, Mater. Lett. 89 (2012) 254.
[18] S. Matsuo, T. Yamada, M. Yoshino, T. Nagasaki, T. Kamo, H. Funakubo, Nonlinear electric field dependence on electrocaloric effect in (001)-epitaxial (Ba,Sr)TiO_3 thin films, in: Joint IEEE International Symposium on the Applications of Ferroelectric (ISAF)/International Workshop on Acoustic Transduction Materials and Devices (IWATMD)/Piezoresponse Force Microscopy (PFM), 2017, pp. 68–70.
[19] C. Zhao, J. Yang, Y. Huang, X. Hao, J. Wu, Broad-temperature-span and large electrocaloric effect in lead-free ceramics utilizing successive and metastable phase transition, J. Mater. Chem. A 7 (2019) 25526–25536.
[20] K. Şanlı, U. Adem, Electrocaloric properties of $Ba_{0.8}Sr_{0.2}Ti_{1-x}Zr_xO_3$ ($0 \le x \le 0.1$) system: the balance between the nature of the phase transition and phase coexistence", Ceram. Int. 46 (2) (2020) 2213–2219.
[21] G. Canu, G. Confalonieri, M. Deluca, L. Curecheriu, M.T. Buscaglia, M. Asandulesa, N. Horchidan, M. Dapiaggi, L. Mitoseriu, V. Buscaglia, Structure-properties correlations and origin of relaxor behaviour in $BaCe_xTi_{1-x}O_3$, Acta Mater. 152 (2018) 258–268.
[22] M. Acosta, N. Novak, V. Rojas, S. Pantel, R. Vaish, J. Koruza, G.A. Rossetti Jr., J. Rodel, $BaTiO_3$-based piezoelectrics: fundamentals, current status, and perspectives, Appl. Phys. Rev. 4 (2017), 041305.
[23] M. Habib, M. Javid Iqbal, M.H. Lee, D.J. Kim, F. Akram, M. Gul, A. Zeb, I. Ur Rehman, M.-.H. Kim, T.K. Song, Piezoelectric performance of Zr-modified lead-free $BiFeO_3$ -$BaTiO_3$ ceramics, Mater. Res. Bull. 146 (2022), 111571.
[24] A. Simon, J. Ravez, M. Maglione, The crossover from a ferroelectric to a relaxor state in lead-free solid solutions, J. Phys. Condens. Matter. 16 (6) (2004) 963–970.
[25] T.N. Verbitskaya, G.S. Zhdanov, Yu.N. Venevtsev, S.P. Solov'ev, Electrical and X-Ray diffraction studies of the $BaTiO_3$-$BaZrO_3$ system", Sov. Phys. - Crystallogr. (Engl. Transl.) 3 (2) (1958) 182–192.
[26] Z.K. Liu, X. Li, Q.M. Zhang, Maximizing the number of coexisting phases near invariant critical points for giant electrocaloric and electromechanical responses in ferroelectrics, Appl. Phys. Lett. 101 (2012), 082904.
[27] D.-.Y. Lu, M. Toda, M. Sugano, High-permittivity double rare-earth-doped barium titanate ceramics with diffuse phase transition, J. Am. Ceram. Soc. 89 (2006) 3112.
[28] H.-.I. Hsiang, G.-.P. Lai, Microstructure evolution and electric properties with additional amounts of dysprosium ($DyO_{1.5}$) in (BaCa)(TiZr)O_3 ceramics, Mater. Sci. Eng. B 123 (2005) 69.
[29] I. Jankowska-Sumara, D. Sitko, M. Podgorna, M. Pilch, The electromechanical behavior of europium doped BaTiO3, J. Alloys Compd. 724 (2017) 703–710.
[30] S.K. Ghosh, S.K. Rout, S.K. Deshpande, Structural and scaling behavior in relaxor ferroelectric BZT ceramic doped with rare earth europium ion, in: Joint IEEE International Symposium on the Applications of Ferroelectric (ISAF), International Symposium on Integrated Functionalities (ISIF), and Piezoelectric Force Microscopy Workshop (PFM), 2015, pp. 17–20.
[31] G. Nag Bhargavi, T. Badapanda, A. Khare, M.S. Anwar, N. Brahme, Investigation of structural and conduction mechanism of Europium modified $BaZr_{0.05}Ti_{0.95}O_3$ ceramic prepared by solid-state reaction method, Appl. Phys. A 127 (2021) 528.
[32] X. Chou, J. Zhai, H. Jiang, X. Yao, Dielectric properties and relaxor behavior of rare-earth (La, Sm, Eu, Dy, Y) substituted barium zirconium titanate ceramics, J. Appl. Phys. 102 (2007), 084106.
[33] G.K. Wertheim, E.V. Sampamthkumaran, C. Laubschat, G. Kaindl, Final-state effects in the x-ray photoemission spectrum of $EuPd_2P_2$, Phys. Rev. B 31 (1985) 6836.
[34] C. Laubschat, B. Perscheid, W.-.D. Schneider, Final-state effects and surface valence in Eu-transition-metal compounds, Phys. Rev. B 28 (1983) 4342.
[35] D.Y. Lu, T. Koda, H. Suzuki, M. Toda, Structure and Dielectric Properties of Eu-Doped Barium Titanate Ceramics, J. Ceram. Soc. Japan 113 (2005) 721–727.
[36] G. Nag Bhargavi, A. Khare, T. Badapanda, P.K. Ray, N. Brahme, Influence of Eu doping on the structural, electrical and optical behavior of Barium Zirconium Titanate ceramic, Ceram. Int. 44 (2018) 1817–1825.
[37] G. Canu, G. Bottaro, M.T. Buscaglia, C. Costa, O. Condurache, L. Curecheriu, L. Mitoseriu, V. Buscaglia, L. Armelao, Ferroelectric order driven Eu^{3+}photoluminescence in $BaZr_xTi_{1-x}O_3$ perovskite, Sci. Rep. 9 (2019) 6441.
[38] F.M. Tufescu, L. Curecheriu, A. Ianculescu, C.E. Ciomaga, L. Mitoseriu, High-voltage tunability measurements of the $BaZr_xTi_{1-x}O_3$ ferroelectric ceramics, J. Optoel. Adv. Mater. 10 (2008) 1894.
[39] G.H. Haertling, Ferroelectric Ceramics: history and Technology, J. Am. Ceram. Soc. 82 (4) (1999) 797–818.
[40] J.M. Wilson, Minerals review – Barium titanate, Am. Ceram. Soc. Bull. 74 (6) (1995) 106–110.
[41] J.S. Capurso, A.A. Bologna, W.A. Schulze, Processing of laminated $BaTiO_3$ structures for stress-sensing applications, J. Am. Ceram. Soc. 78 (9) (1995) 2476–2480.
[42] L. Padurariu, V-Al. Lukacs, G. Stoian, N. Lupu, L.P. Curecheriu, Scale-dependence dielectric properties in $BaZr_{0.05}Ti_{0.95}O_3$ ceramics, Materials (Basel) 13 (2020) 4386.
[43] M.E. Lines, A.M. Glass, Principles and Applications of Ferroelectrics and Related Materials, Oxford University Press, Oxford, 1977.
[44] D.-.Y. Lu, T. Koda, H. Suzuki, M. Toda, Structure and dielectric properties of Eu-doped barium titanate ceramics, J. Ceram. Soc. Jap. 113 (11) (2005) 721–727.
[45] D. Hennings, A. Schnell, G. Simon, Diffuse Ferroelectric Phase Transitions in Ba$(Ti_{1-y}Zr_y)O_3$ Ceramics", J. Am. Ceram. Soc. 65 (11) (1982) 539–544.
[46] C.E. Ciomaga, M. Viviani, M.T. Buscaglia, V. Buscaglia, L. Mitoşeriu, A. Stancu, P. Nanni, Preparation and characterisation of the Ba(Zr,Ti)O_3 ceramics with relaxor properties, J. Eur. Ceram. Soc. 27 (13–16) (2007) 4061–4064.
[47] Z. Sun, Y. Pu, Z. Dong, Y. Hu, X. Liu, P. Wang, Effect of Zr^{4+} content on the T_C range and dielectric and ferroelectric properties of $BaZr_xTi_{1-x}O_3$ ceramics prepared by microwave sintering Ceram, Int., 40 (2014) 3589–3594.
[48] M. Deluca, C.A. Vasilescu, A.C. Ianculescu, D.C. Berger, C.E. Ciomaga, L. P. Curecheriu, L. Stoleriu, A. Gajovic, L. Mitoseriu, C. Galassi, Investigation of the composition-dependent properties of $BaTi_{1-x}Zr_xO_3$ ceramics prepared by the modified Pechini method, J. Eur. Ceram. Soc. 32 (2012) 3551–3566.

[49] C.E. Ciomaga, R. Calderone, M.T. Buscaglia, M. Viviani, V. Buscaglia, L. Mitoseriu, Relaxor properties of Ba(Zr,Ti)O_3 ceramics, J. Optoelectron. Adv. Mater. 8 (2006) 944.
[50] P. Sateesh, J. Omprakash, G.S. Kumar, G. Prasad, Studies of phase transition and impedance behavior of Ba(Zr, Ti)O_3 ceramics, J. Adv. Diel. 5 (1) (2015), 1550002.
[51] U. Bianchi, J. Dec, W. Kleemann, J.G. Bednorz, Cluster and domain-state dynamics of ferroelectric $Sr_{1-x}Ca_xTiO_3$ (x=0.007), Phys. Rev. B 51 (1995) 8737.
[52] W. Kleemann, The relaxor enigma—Charge disorder and random fields in ferroelectrics, J. Mater. Sci. 41 (2006) 129.
[53] L.P. Curecheriu, L. Mitoşeriu, A. Ianculescu, Tunability properties of the $Pb(Mg_{1/3}Nb_{2/3}O_3)$ relaxors and theoretical description, J. Alloy Compd. 485 (1–2) (2009) 1–5.
[54] Q. Zhang, J. Zhai, L.B. Kong, Relaxor ferroelectric materials for microwave tunable applications, J. Adv. Diel. 2 (1) (2012), 1230002.
[55] R.-.H. Liang, X.-.L. Dong, Y. Chen, F. Cao, Y.-.L. Wang, Dielectric properties and tunability of $Ba(ZrxTi_{1-x})O_3$ ceramics under high DC electric field, Ceram. Int. 33 (6) (2007) 957–961.
[56] N. Horchidan, A.C. Ianculescu, L.P. Curecheriu, F. Tudorache, V. Musteata, S. Stoleriu, N. Dragan, D. Crisan, S. Tascu, L. Mitoseriu, Preparation and characterization of barium titanate stannate solid solutions, J. Alloys Comp. 509 (2011) 4731.
[57] Y. Jia, Y.S. Ju, Direct characterization of the electrocaloric effects in thin films supported on substrates, Appl. Phys. Lett 103 (2013), 042903.
[58] F. Zeng, C. Zhou, C. Zhang, J. Zhang, H. Guo, W. Lu, W. Cai, G. Zhang, H. Zhang, G. Fan, Contribution of ferroelectric and nonferroelectric factors to D-E hysteresis loops of $BiFeO_3$-$BaTiO_3$ ceramics, Mater. Res. Bull. 147 (2022), 111617.
[59] L. Padurariu, C. Enachescu, L. Mitoseriu, Monte Carlo simulations for describing the ferroelectric-relaxor crossover in $BaTiO_3$-based solid solutions, J. Phys. Cond. Matt. 23 (32) (2011), 325901.
[60] P. Gwizd, D. Sitko, I. Jankowska-Sumara, M. Krupska-Klimczak, The electrocaloric effect in $BaTiO_3$: eu ceramics determined by an indirect method, Phase Trans. 94 (3–4) (2021) 192–198.
[61] X.-.D. Jian, B. Lu, D.-.D. Li, Y.B. Yao, T. Tao, B. Liang, J.-.H. Guo, Y.-.J. Zeng, J.-.L. Chen, S.-.G. Lu, Direct measurement of large electrocaloric effect in $Ba(Zr_xTi_{1-x})O_3$ ceramics, ACS Appl. Mater. Interfaces 10 (2018) 4801.